JOURNAL OF MATERIALS SCIENCE **26** (1991) 5067–5074

Transient liquid-phase sintering of ceramic-reinforced Fe-based composites

S. J. YANKEE, B. J. PLETKA
Department of Metallurgical and Materials Engineering, Michigan Technological University, Houghton, MI 49931, USA

The microstructural development of ceramic-reinforced iron-based composites has been studied. The composites were fabricated via powder metallurgy and liquid-phase sintering, a processing route which achieves near-net-shape with good ceramic particulate dispersion. Two matrix alloys were used, Fe–1 wt% C–1 wt% Si and Fe–2 wt% Cu; up to 30 wt% (≈36 vol%) yttria-stabilized zirconia in the form of ~20 μm particles was added to these alloys. The microstructural evolution of these composite materials was studied by examining the densification rate and volume fraction of liquid phase as a function of time. Different particle/matrix interfaces developed in the two composites. A glassy silicon-rich layer formed in the Fe–1C–1Si–YSZ composites and a more limited crystalline layer was found in the Fe–2Cu–YSZ composites.

1. Introduction

The fabrication of iron-based metal matrix composites has been examined in the present study. Common methods of fabricating metal matrix composites have relied on techniques such as hot pressing of pre-alloyed powders or casting techniques; in the former, the consolidated billets must then undergo additional deformation processing operations. As an alternative fabrication method, powder metallurgy processing using elemental powders offers advantages such as easy adjustment of alloy composition and ceramic volume fraction, good particulate dispersion, and near-net shape processing. The latter is an especially important consideration due to the difficulty and expense of machining metal matrix/ceramic composites into final component shape. In addition, widespread utilization of any metal matrix/ceramic composite will require economical processing techniques. Accordingly, the feasibility of using transient liquid-phase sintering (TLPS) as a processing technique for the fabrication of iron-based metal matrix composites has been examined in this paper.

A transient liquid is formed in the TLPS process by the melting of one component or the formation of a liquid from the interdiffusion that takes place on heating (see [1–4] for general reviews of liquid phase sintering). As a result of particle rearrangement or solution–reprecipitation, high densities are obtained in relatively short periods of time at moderate sintering temperatures. In particular, densities are achieved such that the porosity becomes isolated (i.e. closed off). Once this condition is attained, further densification is possible by directly hot isostatically pressing the component. As a consequence, this densification process is particularly well-suited for fabrication of composites containing less than ~ 50 vol% reinforcing phase, i.e. compositions for which the metal matrix is the continuous phase.

Two matrix alloys were selected for this study, Fe–2 wt% Cu and Fe–1 wt% Si–1 wt% C. Copper is a common alloy addition in sintered ferrous materials, and Fe–Cu is an example of a TLPS system in which melting of one component takes place on heating the powder mixture to the sintering temperature. The selection of the Fe–C–Si system was based on the desire to obtain a conventional steel matrix microstructure; the addition of silicon to the Fe–C system was made in order to lower the Fe–C eutectic composition because silicon is an austenite de-stabilizer. The overall result is a greater fraction of liquid at a given carbon concentration. The second matrix alloy is also a system in which interdiffusion among the elemental powders must take place in order to form a liquid. These two alloys thus represent the two different mechanisms by which a liquid can form in liquid-phase sintering. The final compositions of both systems lay in the single-phase austenite region at the selected sintering temperature of 1200 °C. Therefore, the liquid which formed in either system was transient.

The ceramic particulate addition selected for this study was yttria-stabilized zirconia (YSZ). Although SiC or Al_2O_3 are often chosen as the ceramic additions in metal matrix composites, YSZ can have a higher fracture toughness (in monolithic form) than SiC or Al_2O_3 if properly heat treated. For the purposes of this study, YSZ served as a model ceramic oxide particulate addition. A range of composite compositions was selected and is listed in Table I.

2. Experimental procedure

Elemental powders of iron, carbon (graphite), silicon, and copper were obtained from Alfa Products, Dan-

0022–2461/91 $03.00 + .12

TABLE I Composite compositions

YSZ addition to Fe matrix (wt %)	Fe–2Cu system (vol % YSZ)	Fe–1C–1Si system (vol % YSZ)
10	13	12
20	25	24
30	37	35

vers, MA, in the form of nominal − 325 mesh (< 44 μm) powder. Zirconia, partially stabilized with 8 wt % yttria (Y_2O_3), was obtained as nominally 25 μm powder from Magnesium Elektron, Inc., New Jersey. The particle morphologies, sizes, and size distributions are listed in Table II. X-ray diffraction of the as-received YSZ powder indicated that the majority of the powder was the cubic phase with a small amount (~ 5%) of monoclinic phase present.

Sample preparation consisted of the blending of elemental and ceramic powders in the desired proportions using a roller-type blender. Table I contains the weight per cent of YSZ and equivalent volume per cents for the various matrix/YSZ systems studied. Green compacts of the pure matrix and composite compositions were formed by cold unidirectional pressing at 660 MPa. A zinc stearate lubricant was applied to the die walls to minimize longitudinal cracking during ejection from the die.

Specimens were TLPS in high-purity argon at 1200 °C for 1 h and furnace cooled under the argon atmosphere. Experiments in which the samples were sintered in air indicated that severe sample oxidation occurred. The TLPS time and temperature were chosen based on preliminary experiments designed to find the minimum processing conditions necessary to achieve isolated (closed) porosity. Hot isostatic pressing (HIPing) for 3 h at 1110 °C and ≈ 173 MPa in high-purity argon was then carried out.

The formation of the liquid phase and the subsequent compact densification were examined by quenching samples at various stages of the sintering process. Specimens for optical and scanning electron microscopy were prepared using standard techniques. Polishing with a colloidal silica suspension on napped cloth with a heavy downward pressure minimized the pull-out of the YSZ particles. Transmission electron microscope foils of both the matrix and composites were ion milled and examined using a Jeol-100CX, operated at 120 kV. Ion milling was done using a cold stage at approximately − 120 °C to minimize ion damage to the foils.

3. Results and discussion

The development of the matrix and composite microstructures during TLPS will be examined, including the densification rates and the volume fraction of liquid formed during TLPS. As will be shown, the TLPS process also influences the nature of the interfacial region which develops between the matrix and the ceramic phase. These interphase boundaries will be examined in detail because they strongly influence the mechanical properties of the composite materials.

3.1. Matrix microstructures

Representative microstructures of the Fe–2Cu material are shown in Fig. 1a and b in the sintered and sintered plus hot isostatically pressed (HIPed) states, respectively. Liquid-phase sintering in the Fe–Cu system has been extensively studied (see [5] for a review), although the amounts of copper used in commercial alloys typically exceed the 2 wt % used in this study. Even though a transient liquid formed during the sintering process, densities of 98.2% were achieved after sintering for 1 h at 1200 °C, and densities of 99.8% were obtained after HIPing. The porosity present in the microstructure was located in the grain interiors. Significant grain growth occurred during processing because the original average iron powder size was ~ 8 μm while the average grain size after sintering and HIPing was ~ 35 μm. The microstructures also appeared single phase even though the composition lay in a two-phase field. Apparently the cooling rate after sintering or HIPing was sufficient to suppress precipitation of the ε-Cu phase or if precipitation did take place, it was not resolved using either optical or scanning electron microscopy.

The microstructure of the Fe–1C–1Si alloy after sintering is shown in Fig. 2. A fully pearlitic microstructure was obtained despite the presence of 1 wt % each of carbon and silicon. Lower densities after sintering and sintering plus HIPing of 95.1% and 98.7%, respectively, were achieved than with the

TABLE II Powder characteristics

Powder	Particle morphology	Approx. size distribution (μm)	Approx. mean particle size (μm)
Fe	Spherical	< 1–10	8
Si	Angular, fairly equiaxed	< 1–10	3
C	Flakes, some rounded	5–15	10
Cu	Rounded, somewhat elongated, agglomerated fines	5–30	20
YSZ	Rounded "raspberry' appearance	15–30	20

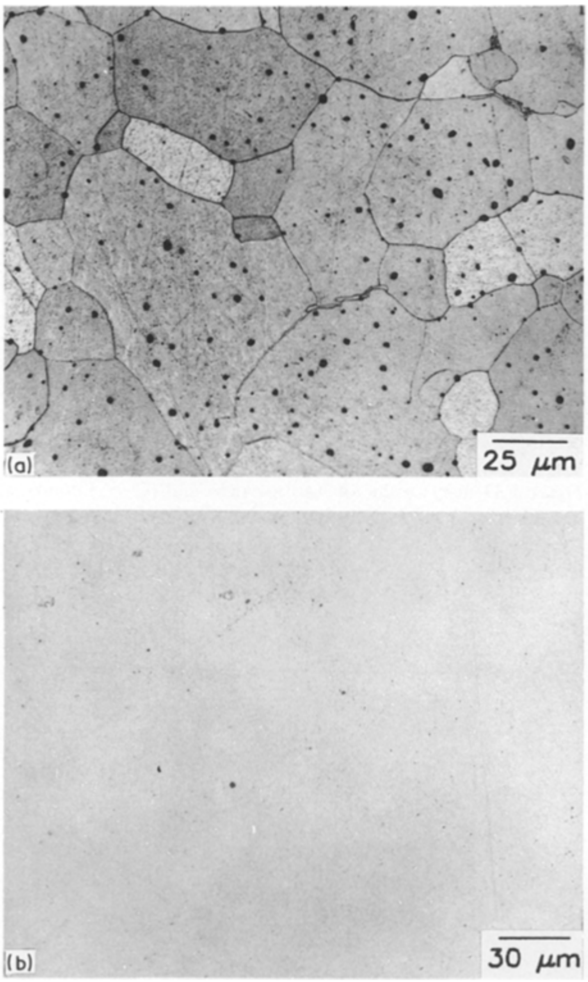

Figure 1 Optical micrographs of the (a) sintered and (b) sintered plus hot isostatically pressed Fe–2Cu matrix.

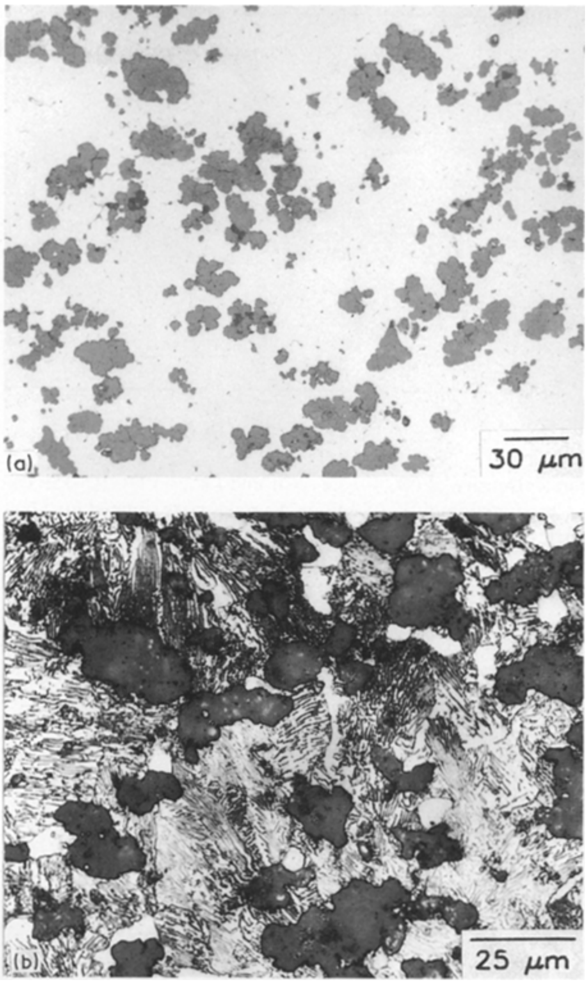

Figure 3 Optical micrographs of the sintered and HIPed (a) Fe–2Cu and (b) Fe–1C–1Si composites containing 20 wt % YSZ.

Fe–2Cu alloy. The lower densities indicate that liquid spreading is more difficult in the Fe–C–Si system than in the Fe–Cu alloy.

3.2. Composite microstructures

Representative composite microstructures are shown in Fig. 3 after sintering and HIPing for materials containing 20 wt % YSZ. In the Fe–2Cu–20YSZ composite, the remaining porosity appears to be located primarily at particle/matrix boundaries (Fig. 3a), while the porosity appears to be distributed both within the matrix and at particle/matrix interfaces for the Fe–1C–1Si–20YSZ composite. The nature of the wetting and structure at the particle/matrix interface is crucial for optimum composite properties and will be investigated in more detail in the next section. The overall development of the composite structure will be examined in this section.

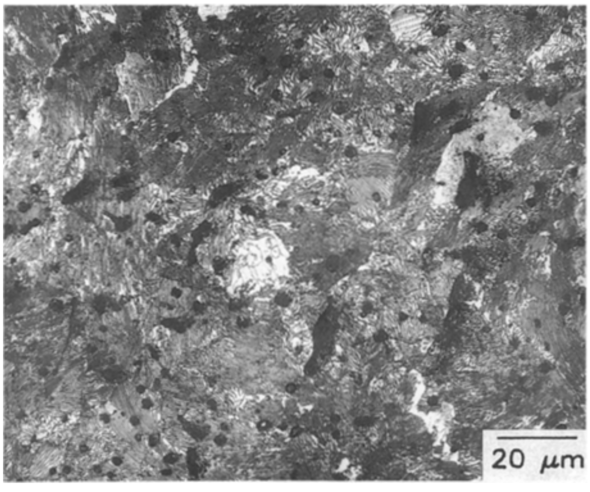

Figure 2 Optical micrograph of the sintered Fe–C–Si matrix.

Final sample densities achieved with TLPS and with TLPS/HIPing, as a function of YSZ content, were determined via point counting. The data were collected from polished surfaces using approximately 6000 grid points per density measurement. The data (Fig. 4) indicate that the final density after TLPS decreased as the YSZ content increased for both of the matrix systems. A similar trend was observed in the HIPed samples, although higher overall density levels were achieved. The decrease in density with YSZ additions was attributed to a lower green density as the YSZ content was increased and to increasing porosity which formed at the particle/matrix interfaces. For example, the green density of the Fe–2Cu alloy was ~ 75% theoretical, but only about 69% in the Fe–2Cu–20YSZ composite. Similarly for the

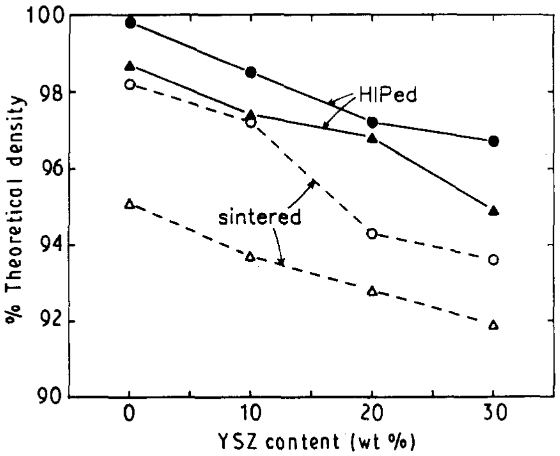

Figure 4 Density of (●, ○) Fe–2Cu and (▲, △) Fe–1C–1Si systems as a function of YSZ addition. Samples were sintered for 1 h at 1200 °C in high-purity argon, then HIPed for 3 h at 1110 °C and 173 MPa.

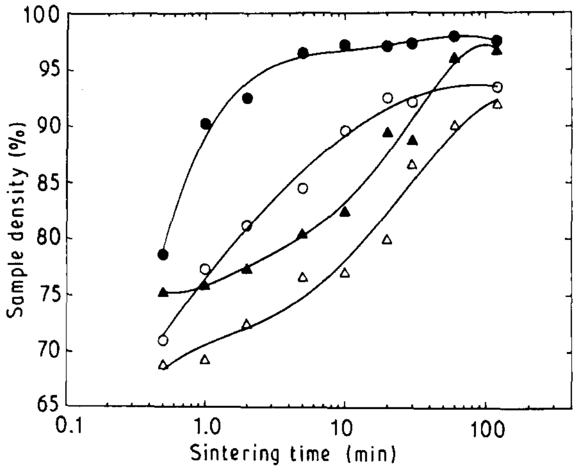

Figure 5 Density of the (●, ▲) matrices and (○, △) composites (containing 20 wt % YSZ) as a function of time at the sintering temperature of 1200 °C. (●) Fe–2Cu, (○) Fe–2Cu–20YSZ, (▲) Fe–1C–1Si, (△) Fe–1C–1Si–20YSZ.

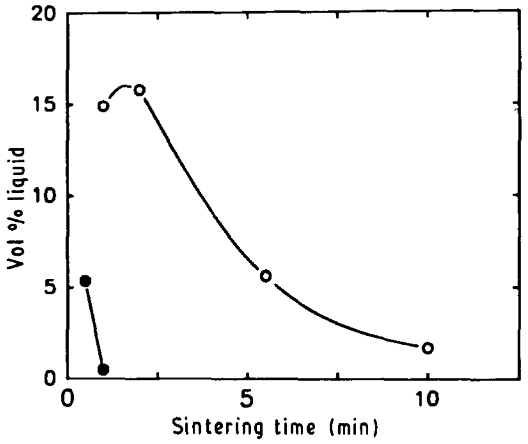

Figure 6 Volume fraction of liquid formed as a function of time at 1200 °C in composites containing 20 wt % YSZ: (●) Fe–2Cu–20YSZ, (○) Fe–1C–1Si 20YSZ.

Fe–C–Si system, the green density of the matrix alloy was about 74% while the Fe–C–Si–20YSZ composite was only ~ 67%.

In order to understand the densification process during TLPS of these materials, specimens were quenched after being held for various times (30 s–120 min) at the sintering temperature of 1200 °C. These experiments involved the matrix alloys and a composite composition from each matrix system. The densities as a function of sintering time at 1200 °C are plotted in Fig. 5. With the exception of the Fe–1C–1Si–20YSZ samples, data were collected via point counting; densities were obtained for the former by measuring sample mass and volume due to the difficulty in avoiding particle pull-out during polishing of the lower density specimens. An empirical correction based on the point-counted data for the other compositions was applied to the Fe–1C–1Si–20YSZ so that all density data could be compared directly. It can be observed that different densification rates exist between the two matrix systems. Specifically, densification is initially very rapid in the Fe–2Cu matrix samples but the density becomes nearly constant after ≈ 10 min at 1200 °C. In contrast, the Fe–1C–1Si matrix samples exhibited a sigmoidal-shaped densification rate (slow densification early and late in the densification cycle but rapid at intermediate times). The data also indicate that similar rates of densification exist between the composites and their respective matrices. This is not surprising because the presence of YSZ within a given matrix would not be expected to greatly change the densification kinetics of the matrix material unless appreciable solubility of the particulate in the liquid was possible.

The volume fraction of liquid was also studied as a function of sintering time in order to obtain a better understanding of the different densification kinetics observed between the two matrix systems. These data, shown in Fig. 6, were collected by point counting polished surfaces of quenched samples. The data indicate that a smaller volume fraction of liquid developed in the Fe–2Cu system. The liquid was also present for a much shorter period of time at 1200 °C. It is important to recognize, however, that melting of the copper particles took place at ~ 1085 °C as the green compacts were heated to the sintering temperature of 1200 °C. Therefore, formation of the liquid on heating resulted in rapid homogenization and disappearance of the liquid, consistent with the densification rates observed in Fig. 5. Interdiffusion and higher temperature are required for the liquid to form in the Fe–1C–1Si matrix samples, and these factors account for the slow initial densification rate which then increased as the fraction of liquid increased at 1200 °C.

Further evidence of the role the liquid plays in densification during TLPS was obtained from a log–log plot of per cent shrinkage (densification) versus sintering time. Shrinkage was defined as

$$\% \text{ shrinkage} = (\rho_s - \rho_g)/\rho_g \qquad (1)$$

where ρ_s and ρ_g are the sintered and green densities, respectively. From classical coarsening theory, a slope (time dependence) of one-third on such a plot would indicate that solid-state diffusion mechanisms control the densification. Exponents of magnitude greater than one-third would indicate, however, that accelerated densification mechanisms such as particle rearrangement or solution-reprecipitation were active [6, 7]. The density data obtained from the quenching experiments for the Fe–2Cu specimens (Fig. 7a) indicate that the slope, or time dependence, is very close to one-third. This means that solid-state diffusion was the dominant densification mechanism during the time period studied. This observation is consistent with the results in Figs 5 and 6 and emphasizes the rapid formation and disappearance of the liquid phase during TLPS in the Fe–2Cu system. In contrast, the Fe–1C–1Si data in Fig. 7a display a distinct break in the curve. This indicates a change in densification mechanism takes place, such as solution-reprecipitation to solid-state processes. The change in mechanism also corresponds to the time period at which the maximum volume fraction of liquid was attained. Similar density plots were obtained for the composite specimens (Fig. 7b) indicating that the presence of YSZ does not significantly affect the densification kinetics of the matrix materials.

An important factor which influences the properties of composite materials is the dispersion or homogeneity of the reinforcing phase obtained during processing. In order to assess whether particle clustering was present in the composite microstructures, the contiguity ratio, C_t, was determined for each composite material. This parameter describes the degree to which particles touch and can have values which vary from 0–1 as the phase of interest varies from fully dispersed to fully agglomerated [8]. Measurements were made following standard practices and the data are plotted in Fig. 8; a ratio of ≈ 0.2 was attained at all levels of particulate reinforcement. This indicates that $\approx 20\%$ of the total particle surface area is contacted by other YSZ particles. The particle clustering observed in these composites will have an effect on the composite mechanical properties.

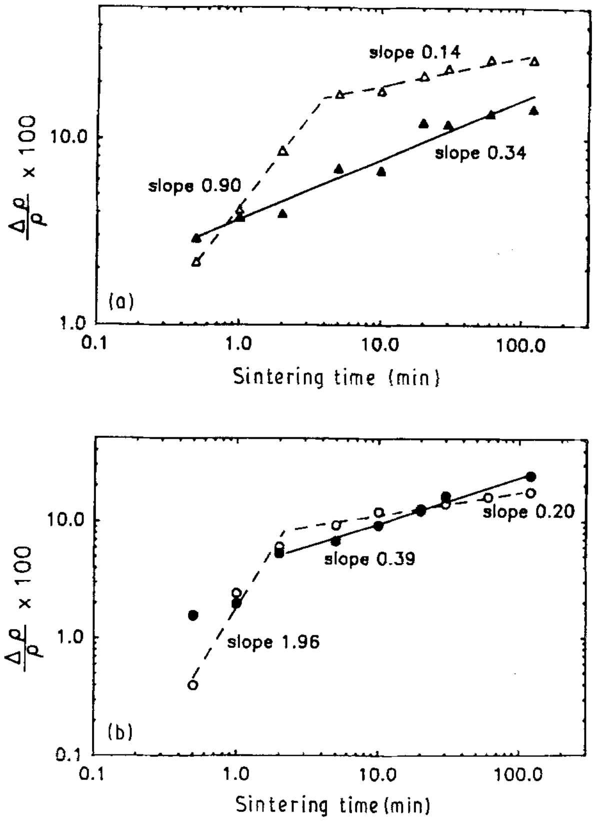

Figure 7 Log of the densification (shrinkage) as a function of log time for (a) the matrix materials, and (b) the composites containing 20 wt % YSZ. (▲) Fe–2Cu, (△) Fe–1C–1Si, (●) Fe–2Cu–20YSZ, (○) Fe–1C–1Si–20YSZ.

3.3. Interfacial structures

The interface between the metal matrix and the reinforcing phase in composite materials is a critical region of the microstructure, because the interface "quality" largely determines whether the load is transferred from the matrix to the ceramic phase. These regions were studied in detail in both composite systems.

3.3.1. Fe–C–Si–YSZ composites

Examination of the as-processed microstructures after normal metallographic preparation via optical microscopy or SEM did not reveal distinct layers or particles present at the ceramic/matrix interfaces. However, after TEM foils were prepared by ion milling, it was observed that a region approximately 2–3 μm thick surrounding the YSZ particles in the Fe–1C–1Si–YSZ composites was ion milled preferentially. An example of this interfacial region is shown in the scanning electron micrograph in Fig. 9a. A typical electron diffraction pattern from this region (Fig. 9b) displays diffuse rings of intensity maxima, indicating an amorphous material is present. Centred dark-field (CDF) imaging using the innermost intensity maxima (see double-exposed aperture position in Fig. 9b) produced the micrograph in Fig. 9c; only those regions ion milled preferentially are in contrast, confirming the non-crystalline nature of the interfacial regions. CDF imaging at lower magnification substantiated that these regions surrounded many particles. It is

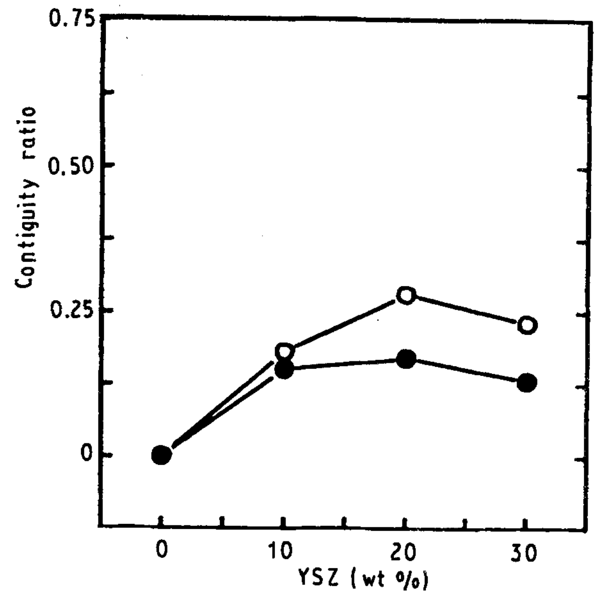

Figure 8 Contiguity ratio (which indicates particle touching) as a function of YSZ content in (●) Fe–2Cu and (○) Fe–1C–1Si systems.

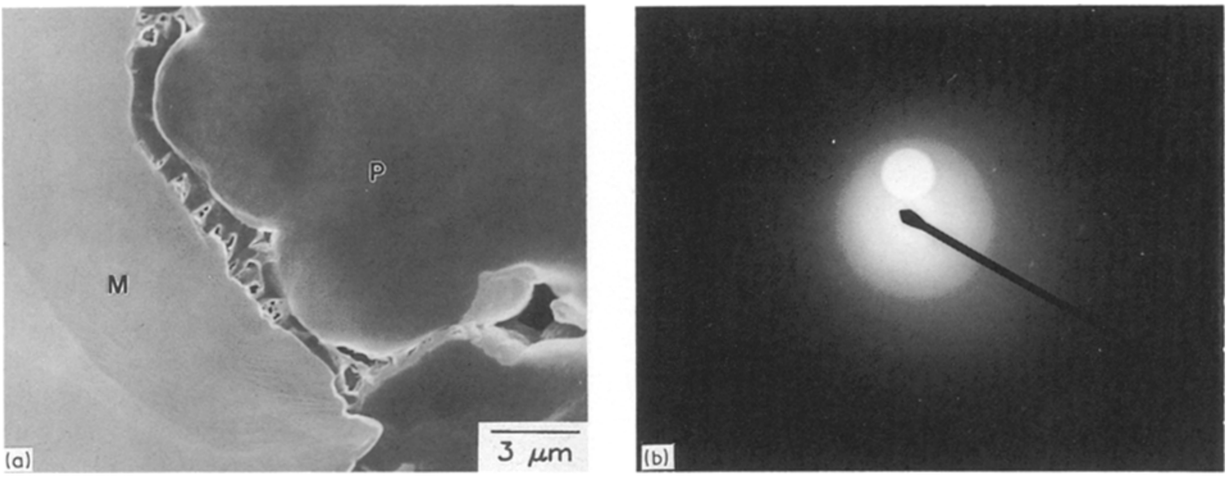

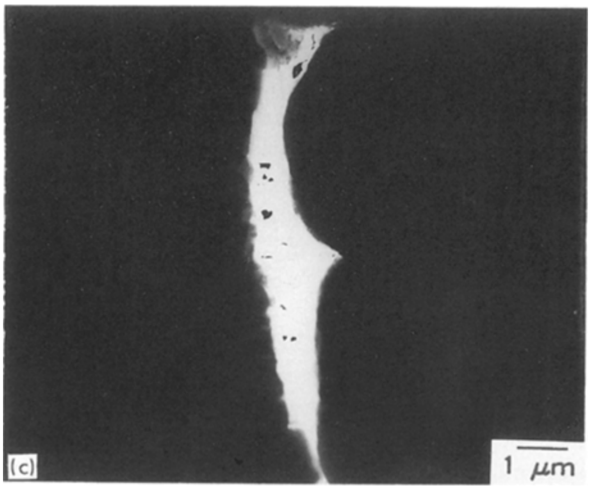

Figure 9 (a) Scanning electron micrograph of the preferentially ion-milled interface between a YSZ particle (P) and the matrix (M). (b) Electron diffraction pattern from the interfacial region shown in (a), with the position of the objective aperture used for dark-field imaging also shown. (c) Centred dark-field image using the diffracted intensity indicated in (b).

believed that the glass was formed during processing of the Fe–1C–1Si–YSZ system and did not result from ion milling, because ion-milled Fe–2Cu–YSZ composites did not show evidence of glass formation.

Qualitative chemical analysis of the glassy regions was obtained via X-ray mapping. Fig. 10b and 10c illustrate typical maps for silicon and oxygen, respectively, of a YSZ particle and the surrounding matrix material. A scanning electron micrograph of the same area is shown in Fig. 10a for reference. Comparison of the micrographs indicates a substantial enrichment of silicon occurred in the interfacial region(s) and there is some suggestion of oxygen enrichment. Attempts to obtain X-ray maps of carbon were unsuccessful due to the low atomic number of carbon and consequent high absorption. However, based on the qualitative results of the silicon and oxygen X-ray maps, it is suggested that the interfacial regions are composed of a silicon-rich glass. Chemical microanalysis was also performed using EDS via STEM on ten random points within a glassy region surrounding an individual particle. Standardless thin film analyses yielded results for iron, silicon and zirconium, given in Table III. The average silicon concentration is seen to be considerably greater than the ~ 2 at % Si originally added to the matrix. The wide variation in the data, due in part to a non-uniform sample thickness, precludes using the data in a quantitative manner. The significant enrichment of silicon in the glassy region is confirmed, however, by these data.

From the chemical analyses at the particle/matrix interface, it is believed that the silicon-rich liquid segregates to the YSZ particles. The segregation may be a result of the reduced ability of the liquid to wet the iron particles in the Fe–C–Si system (compare the density data for the matrix alloys in Fig. 4). Consequently, the liquid delivers to the particle/matrix interface a relatively large proportion of the total silicon present in the sample. Furthermore, the presence of a silicon-rich glassy layer around YSZ particles implies that an equilibrium exists between these phases. Kagawa *et al.* [9] have studied plasma-sprayed ZrO_2 and SiO_2 powders. They observed that ZrO_2 precipitated first from the plasma and SiO_2 deposited as a coating on the ZrO_2 particle surfaces. These results support the idea that a SiO_2 layer preferentially forms around YSZ particles in the TLPS composites if similar phase equilibria exist between SiO_2 and yttria-stabilized zirconia.

The effect of silicon on the development of glassy interfaces is not limited to iron-based composites. Janowski and Pletka [10] have shown that a glassy interfacial region is present in liquid-phase sintered silicon-containing aluminium alloys reinforced with Al_2O_3. This suggests that silicon in the presence of an oxide may lead to the formation of amorphous interfacial regions regardless of the matrix material.

3.3.2. Fe–Cu–YSZ composites

The interfacial regions in a Fe–2Cu–20YSZ foil having a comparable fabrication history to the Fe–1C–1Si–YSZ samples were also examined. An example of the observed particle/matrix interfacial regions is shown in Fig. 11a. A light-coloured interfacial layer is present, although it is of considerably lesser extent than in the Fe–1C–1Si–YSZ samples. Attempts to identify the exact nature of the interfacial layer were unsuccessful. No evidence was found to suggest, however, that these layers were glassy. It is not surprising

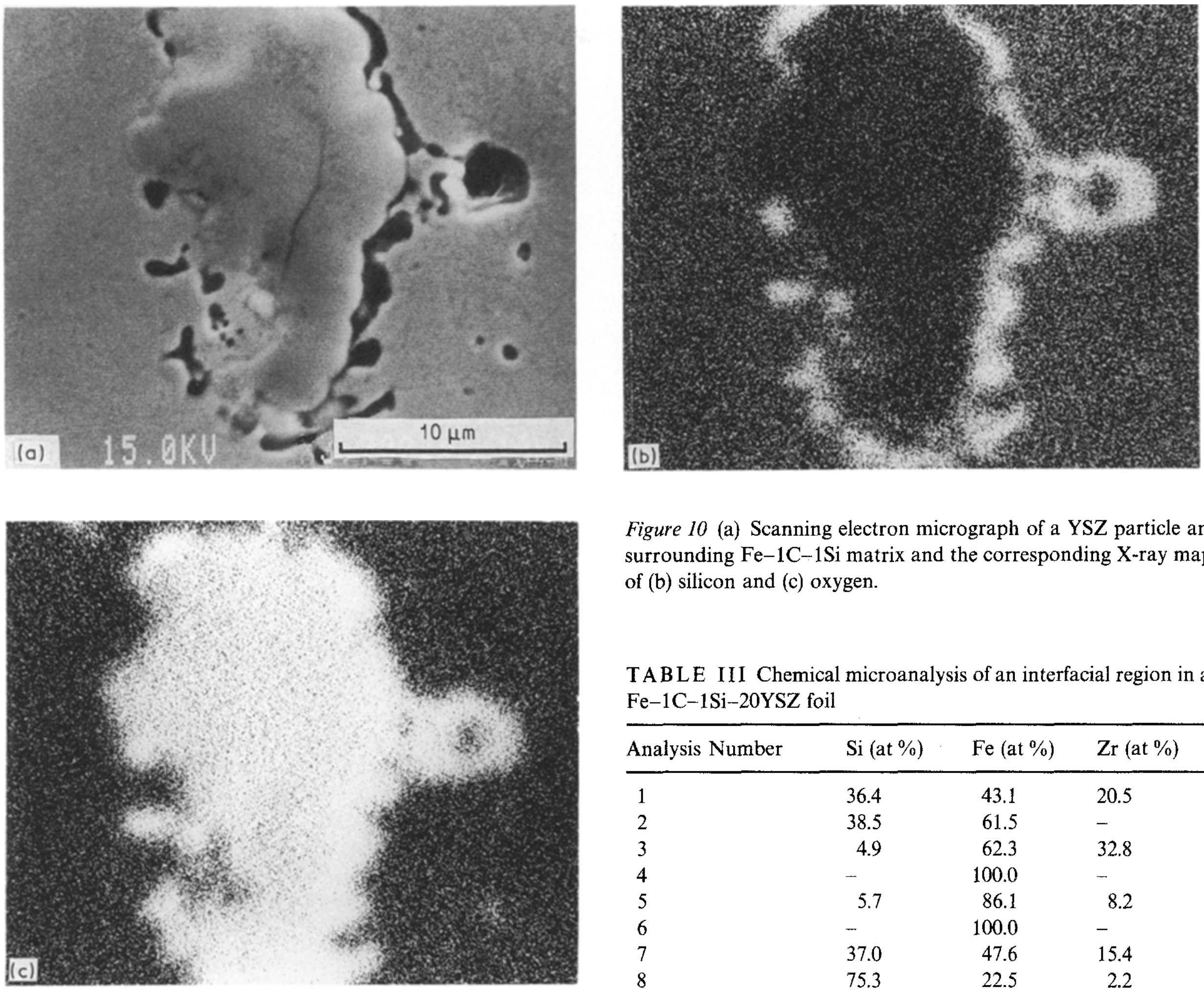

Figure 10 (a) Scanning electron micrograph of a YSZ particle and surrounding Fe–1C–1Si matrix and the corresponding X-ray maps of (b) silicon and (c) oxygen.

TABLE III Chemical microanalysis of an interfacial region in an Fe–1C–1Si–20YSZ foil

Analysis Number	Si (at %)	Fe (at %)	Zr (at %)
1	36.4	43.1	20.5
2	38.5	61.5	–
3	4.9	62.3	32.8
4	–	100.0	–
5	5.7	86.1	8.2
6	–	100.0	–
7	37.0	47.6	15.4
8	75.3	22.5	2.2
9	4.7	94.1	1.2
10	61.3	32.3	6.4

that a glassy interfacial region would not be observed in this system, because the formation of a copper-rich glass would require a cooling rate much faster than that achieved by furnace cooling.

Fig. 11a also indicates that the liquid apparently penetrated the YSZ grain boundaries during TLPS. The diffusional nature of this penetration is illustrated by the lower magnification micrograph in Fig. 11b, in which the central region of the YSZ particle has not undergone grain-boundary penetration. This phenomenon was not observed in the Fe–1C–1Si–YSZ specimens. It appears, therefore, that the copper-rich liquid wets the YSZ particles to a greater extent than the liquid in the Fe–C–Si system. This observation is consistent with previous work in which it was found that a eutectic or near-eutectic liquid of Cu–O, which forms under appropriate oxygen partial pressures, will wet oxide ceramics such as Al_2O_3 and ZrO_2 [11]. In addition, recent work by Nogi *et al.* [12] has demonstrated extensive penetration of ZrO_2 by liquid copper when a d.c. voltage is applied to the system to control the migration of oxygen ions (i.e. oxygen concentration) at the ceramic/liquid metal interface. The penetration behaviour observed in the present study is also consistent with greater densification being achieved in the Fe–Cu–YSZ composites at a given volume fraction of particulate addition.

4. Conclusion

Transient liquid-phase sintering of pressed elemental powders at 1200 °C for 1 h has been found to result in densities exceeding 92% theoretical for composites containing less than 37 vol % particulate YSZ. Densities ranging from 95%–98.5% theoretical were achieved in the composites after hot isostatic pressing at 1110 °C and 173 MPa. Similar rates of densification were found for the composite materials and the corresponding matrix alloy. Some particle clustering and porosity which formed at the particle/matrix interface were observed in the composites; these microstructural features will affect the mechanical properties of the composites.

The Fe–1C–1Si–YSZ and Fe–2Cu–YSZ composites were found to possess different types of particle/matrix interfacial regions. A silicon-rich glassy region was confirmed around the particles in the Fe–C–Si–YSZ composites from TEM studies and X-ray mapping analysis. An apparently crystalline layer of more limited extent was detected in the Fe–Cu–YSZ composites. Penetration of the YSZ particulate grain boundaries by the copper-rich liquid was noted, but no similar phenomenon was found in the Fe–C–Si–YSZ composites. This observation supports the greater extent of wetting and densification observed in the Fe–Cu–YSZ composites compared to the Fe–C–

Si–YSZ composites.

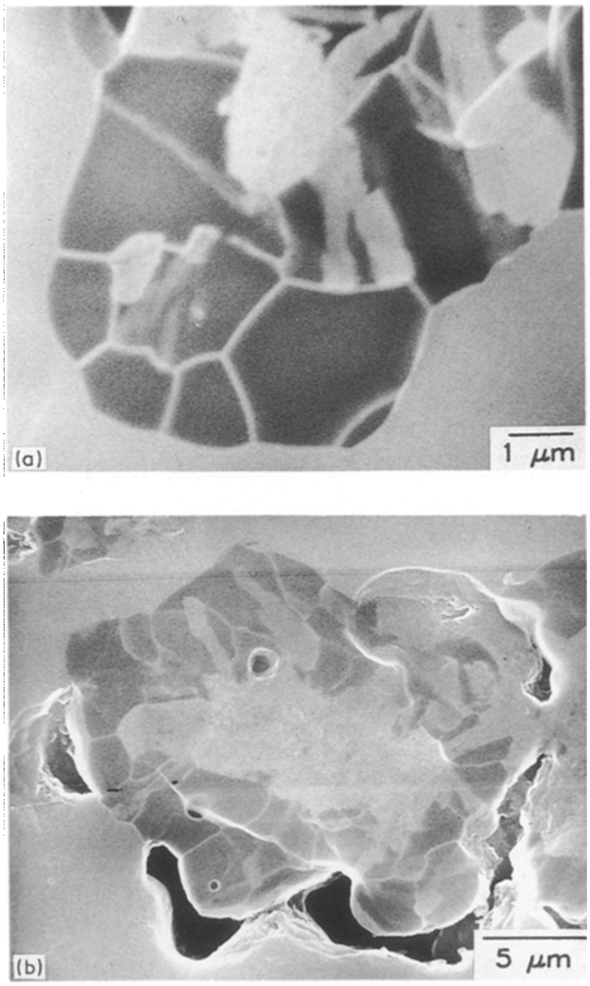

Figure 11 (a) Scanning electron micrograph of a YSZ particle in an Fe–2Cu matrix illustrating the penetration of the liquid along the YSZ particle grain boundaries and the formation of a layer at the particle/matrix interface. (b) Lower magnification micrograph of another YSZ particle demonstrating the diffusional nature of the liquid penetration.

Acknowledgements

The authors thank Teledyne Continental, Inc., General Products Division, for partial support of this work. Additional support for S. J. Yankee was provided by the Department of Metallurgical and Materials Engineering at Michigan Technological University. The authors also thank G. M. Janowski for assistance with electron microscopy.

References

1. G. PETZOW and W. A. KAYSSER, in "Sintered Metal-Ceramic Composites", edited by G. S. Upadhyaya (Elsevier Science, Amsterdam, 1984) p. 51.
2. T. H. COURTNEY, *Metall. Trans.* **15A** (1984) 1065.
3. R. M. GERMAN, *J. Metals* **38** (1986) 26.
4. R. M. GERMAN, "Liquid Phase Sintering" (Plenum Press, New York, London, 1985).
5. R. M. GERMAN and K. A. D'ANGELO, *Int. Metals Rev.* **29** (1984) 249.
6. W. J. HUPPMANN, in "Sintering and Catalysis", edited by G. C. Kuczynski (Plenum Press, New York, London, 1975) p. 359.
7. W. D. KINGERY and M. D. NARASHIMHAN, *J. Appl. Phys.* **30** (1959) 307.
8. J. GURLAND, in "Quantitative Microscopy" (McGraw-Hill, New York, 1968) p. 278.
9. M. KAGAWA, Y. SYONO, Y. IMAMURA and S. USUI, *J. Amer. Ceram. Soc.* **69** (1986) C50.
10. G. M. JANOWSKI and B. J. PLETKA, *Mater. Sci. Engng,* **A129** (1990) 65.
11. J. F. BURGESS, C. A. NEUGEBAUER and G. FLANAGAN, *J. Electrochem. Soc.* **122** (1975) 688.
12. K. NOGI, H. TAKEDA and K. OGINO, *Mater. Trans. Jpn. Inst. Metals* **31** (1990) 83.

Received 23 July 1990
and accepted 24 January 1991